Journal of Nuclear Materials 176 & 177 (1990) 110–121
North-Holland

Structures for handling high heat fluxes *

R.D. Watson

Sandia National Laboratories, Fusion Technology Division 6428, P.O. Box 5800, Albuquerque, NM 87185, USA

The divertor is reconized as one of the main performance limiting components for ITER. This paper reviews the critical issues for structures that are designed to withstand heat fluxes > 5 MW/m^2. High velocity, sub-cooled water with twisted tape inserts for enhanced heat transfer provides a critical heat flux limit of 40–60 MW/m^2. Uncertainties in physics and engineering heat flux peaking factors require that the design heat flux not exceed 10 MW/m^2 to maintain an adequate burnout safety margin. Armor tiles and heat sink materials must have a well matched thermal expansion coefficient to minimize stresses. The divertor lifetime from sputtering erosion is highly uncertain. The number of disruptions specified for ITER must be reduced to achieve a credible design. In-situ plasma spray repair with thick metallic coatings may reduce the problems of erosion. Runaway electrons in ITER have the potential to melt actively cooled components in a single event. A water leak is a serious accident because of steam reactions with hot carbon, beryllium, or tungsten that can mobilize large amounts of tritium and radioactive elements. If the plasma does not shutdown immediately, the divertor can melt in 1–10 s after a loss of coolant accident. Very high reliability of carbon tile braze joints will be required to achieve adequate safety and performance goals. Most of these critical issues will be addressed in the near future by operation of the Tore Supra pump limiters and the JET pumped divertor. An accurate understanding of the power flow out of edge of a DT burning plasma is essential to successful design of high heat flux components.

1. Introduction

The function of high heat flux components is to remove both heat and particle fluxes, as well as to pump impurities, in a safe, reliable, and cost effective manner without contaminating the plasma. However, because of the severe environment and uncertainties in plasma edge conditions, future designs may have difficulties meeting these requirements. With the recent attainment of long pulse, high power operation in tokamak fusion devices, plasma facing components (PFCs) such as first wall tiles, limiters, RF antennae, and divertors need to be actively cooled. Active cooling is required for pulse lengths greater than 10 s, and heat fluxes greater than 5 MW/m^2 [1]. Although most large machines do not require active cooling of PFCs (DIII-D, TFTR, JT-60, and CIT), others have already installed water cooled components, including ASDEX, ASDEX-Upgrade, and Tore Supra. JET plans to add a water cooled pumped divertor system in 1992. Use of active cooling generates a whole new set of problems that must be solved, including: bonding, materials selection, thermal-hydraulics, thermo-mechanics, response to runaway electrons, safety and reliability issues. Successful operation of these components depends critically on understanding better the plasma–wall interactions and aggressive environment in which these structures operate.

2. Operating conditions

Surface heat loads are generated by ion and electron impact, as well as electromagnetic radiation. The largest contribution is from ion and electron impact, although new designs for high-recycling, radiating divertors will have a larger contribution from electromagnetic radiation. Nuclear heating adds only a small fraction to the total heating. Table 1 lists typical operating parameters. It is interesting to note that these heat fluxes are significantly higher than previous values for INTOR, FED, and STARFIRE (2–4 MW/m^2), because of more accu-

* This work was performed at Sandia National Laboratories and was supported by the US Department of Energy under Contract DE-AC04-76DP00789.

0022-3115/90/$03.50 © 1990 – Elsevier Science Publishers B.V. (North-Holland)

Table 1
Operating conditions for high heat flux plasma facing

Machine	Component	Heat flux MW/m^2	Pulse length
Tore supra	Pump limiter	30	30
ASDEX	Divertor	3	5
ASDEX-Upgrade	Divertor	3–5	10
JET	Pumped divertor	15 (includes sweeping)	10
FER	Divertor	10	2000
ITER/NET	Divertor	15	200–1000

rate plasma edge models, and a more realistic assessment of heat flux peaking factors [2].

3. Design options

High heat flux structures must use thin wall sections to keep temperatures within acceptable limits. Fig. 1 shows four possible cross-sections for the ITER divertor [3,4]. Typical dimensions are 5–10 mm for the armor tile and 1–3 mm for the heat sink wall thickness. A strong metallurgical bond (brazing, diffusion bonding, etc.) is required in these duplex structures to transfer heat efficiently across the interface. Braze alloys containing small amounts of titanium (1–10%) are used to promote wetting of graphite by forming titanium carbide at the interface [5]. Design No. 1 is the best developed of the four, and utilizes a double containment of the coolant. Molybdenum was chosen because of its high melting point, and because of its good expansion match to carbon fibre composites (CFC). Design No. 2 eliminates the secondary containment and brazes the tubes directly into the carbon armor tile (e.g., "monoblock"). This simplifies fabrication. Design No. 3 uses double containment with a dispersion strengthened copper alloy for the heat sink. This requires an intermediate bonding interlayer (such as molybdenum) between the tile and substrate because of the large expansion mismatch between copper and CFCs. Design No. 4 uses beryllium tiles either brazed or plasma sprayed on to a copper alloy heat sink with double containment. To date, only designs Nos. 1 and 3 have been tested, although the other two should be tested soon.

One of the candidate divertor elements for Asdex-Upgrade uses CL-1116 PT isotropic graphite brazed to a molybdenum alloy (TZM) heat sink made by Plansee, Austria with a counter-flow cooling design. These elements were tested at 7 MW/m^2 for 3000 cycles, 60 s pulses, without failure [6,7]. Fig. 2 shows the Tore Supra pump limiter elements designed by CEA, France. The armor tiles consist of CL-1116 PT on the sides and CL Aerolor A05 CFC on the tip, each brazed to a Cu–Cr–Zr alloy counterflow element with a twisted tape insert for enhanced heat transfer. These elements were tested to 10 MW/m^2 for 100, 30 s pulses without failure.

The proposed JET pumped divertor elements consist of a water cooled hypervapotron unit made of a Cu–Cr–Zr alloy with 3 mm thick beryllium tiles brazed on to the surface [8]. Hypervapotron units, which have been operated extensively as neutral beam dumps in JET, operate well at 10 MW/m^2, and are currently being tested to 15 MW/m^2. Because of the transverse internal fins, this design benefits from using a low water

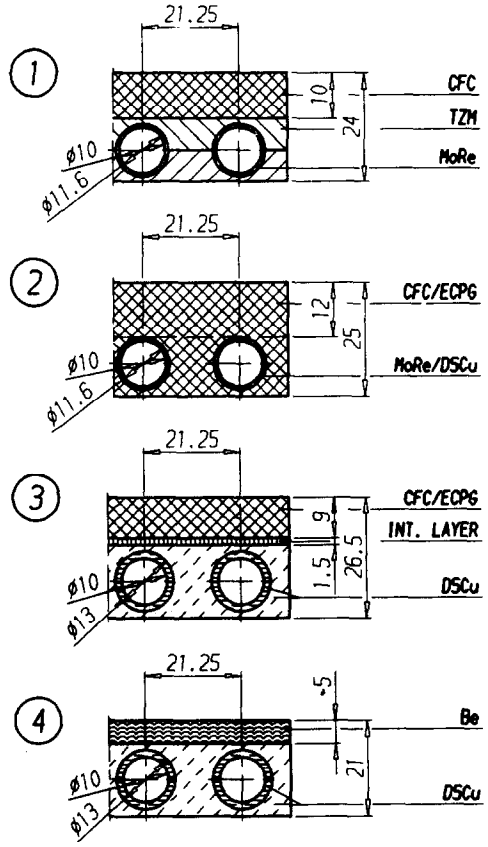

Fig. 1. Actively cooled divertor designs proposed for ITER. CFC = carbon fibre composite, ECPG = extremely conductive pyrolytic graphite, DSCu = dispersion strengthened copper alloy (dimensions in mm).

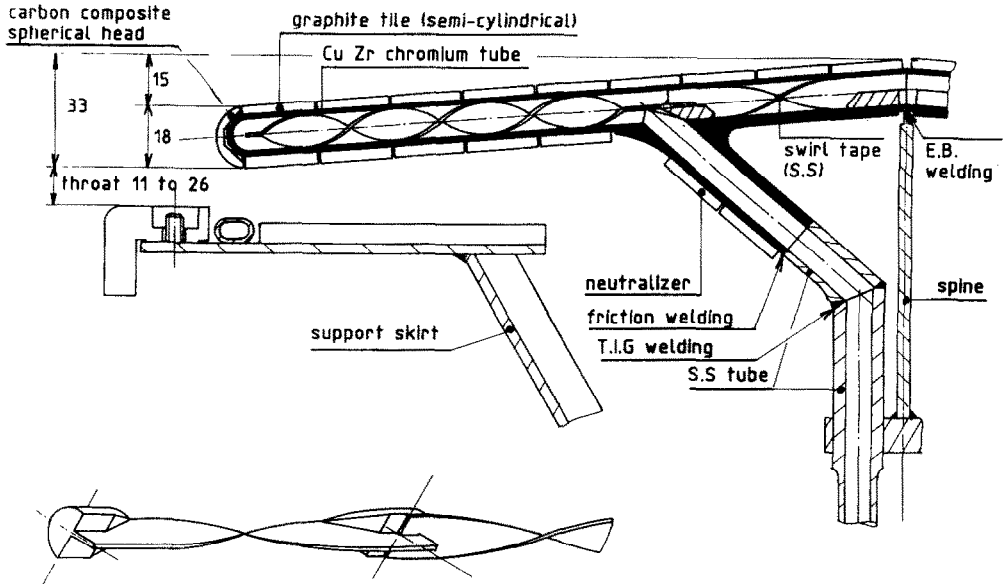

Fig. 2. Cross-section of Tore Supra pump limiter cooling tube designed by CEA, Cadarache, France showing swirl counter-flow twisted tape insert for enhanced heat transfer.

pressure, low flow rate, and low pressure drop. However, oscillating boiling phenomena between the fins cause large vibrations to occur.

A proposed design for the ITER Physics Phase divertor used 10 mm thick CFC tile brazed to an 18 mm diameter oxide dispersion strengthened copper alloy tube in the monoblock geometry [9]. Advantages of the monoblock design include: reduction of residual braze stresses by elimination of the stress singularity at the free edge corner, easier brazing (self-jigging), greater tolerance to braze melting from off-normal events, and greater tolerance of braze defects. For the ITER Technology Phase, a 2 mm thick tungsten tile is brazed or plasma sprayed on to a 2 mm thick Nb–1Zr alloy plate with rectangular coolant channels. A flow constriction is used to enhance the heat transfer coefficient under-

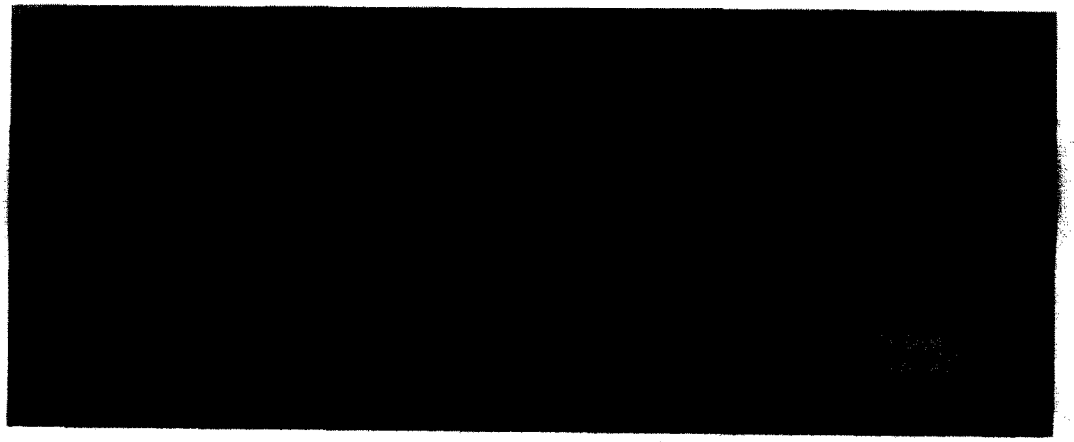

Fig. 3. Prototype ITER divertor element. 3 mm thick beryllium is is plasma sprayed on to OFHC copper block, which is brazed to an oxide dispersion strengthened copper alloy tube. Slots in beryllium are used to reduce thermal stresses.

neath the strike point by locally increasing the water velocity from 10 to 16 m/s. Fig. 3 shows a prototype divertor element that has 3 mm of plasma sprayed beryllium sprayed on to an OFHC copper interlayer, which is brazed to a dispersion strengthened copper alloy cooling tube. Electron beam testing of this target is scheduled for June, 1990 at Sandia National Laboratories.

The highest steady-state heat flux levels reached for a duplex HHF component is the phase III pump limiter for Tore Supra [10]. 10 mm thick pyrolytic graphite tiles are brazed to a 10 mm diameter OFHC copper tube with twisted tape insert. This design has survived 30 MW/m^2 for 1000 cycles with 30 s pulses, without any damage to the tiles [11].

4. Materials selection

Desirable properties for the plasma facing materials include: high thermal conductivity, low Z, good thermal shock resistance, low sputtering, low coefficient of thermal expansion (CTE), low elastic modulus, high melting point, high strength, high toughness, low outgassing, low tritium inventory, low neutron activation, good oxidation resistance, low toxicity, low swelling and embrittlement, low cost, etc. However, the selection of

Table 2
Comparison of plasma facing materials properties

Property (at 600 °C)	CFC	PG/CAPG	Beryllium	Tungsten
Thermal conductivity	100–300 W/mK	300/500 W/mK	100 W/mK	140 W/mK
Thermal shock resistance	excellent	delaminates	good	microcracks
Melting point	(2500°C)	(2500°C)	1283°C	3410°C
Density	1.8–2.0 g/cm^3	2.2 g/cm^3	1.85 g/cm^3	19.2 g/cm^3
Heat capacity	1.6 J/g K	1.6 J/g K	2.3 J/g K	1.4 J/g K
Atomic number	6	6	4	74
D-sputtering, 50 eV	0.008	0.008	0.002	$\ll 1\times10^{-3}$
D-sputtering, 200 eV	0.02	0.02	0.02	2×10^{-5}
Chemical sputtering	yes	yes	?	?
Radiation enhanced sputtering	yes	yes	?	?
Yield strength	50 MPa	100 MPa	160 MPa	80–1300 MPa
Ultimate strength	50 MPa	100 MPa	200 MPa	400–1400 MPa
Ductility at 25°C	<1%	<1%	3–5%	<1%
Ductility at 400 °C	?	2%	50%	10–50%
Anisotropy	small–large	very high	none	small
Young's modulus	22 GPa	28 GPa	230 GPa	390 GPa
Thermal expansion coefficient (CTE)	1.5×10^{-6}	1.5×10^{-6}	20×10^{-6}	4.3×10^{-6}
CTE match with heat sink	poor with copper good with Mo	poor in $a-b$ plane	excellent with copper	excellent with Mo/Nb
Porosity	5–20%	0	1–2%	0
Tritium inventory	high	low	moderate	moderate
Tritium permeation	very high	very low	low	low
Tritium co-deposition	very large	very large	none ?	none ?
Short term radioactivity	low	low	low	high
Radiation waste management	low	low	low	high
Volativity	low	low	medium	high
Oxidation resistance	low	low	low	low
Decay afterheat	low	low	low	high
Chemical toxicity	low	low	high	low
Plasma spray application	no	no	yes	yes
Protection of heat sink from runaway electrons	poor	poor	poor	good

materials is a particularly challenging task because no one set of materials can adequately satisfy all of the requirements [12]. Promising candidates for armor materials are isotropic graphite, carbon fiber composites (CFC), pyrolytic graphite (PG), compression annealed pyrolytic graphite (CAPG), beryllium, and tungsten. Bonding techniques for armor tiles include brazing, diffusion bonding, and plasma spray coating.

Table 2 summarizes the materials properties of carbon, beryllium, and tungsten for use as plasma facing materials. The main disadvantages of carbon are: carbon blooms from radiation enhanced sputtering (RES), low strength, low fracture toughness, anisotropic (PG/CAPG), poor CTE match with copper, difficult to bond PG/CAPG, high porosity of CFCs, outgassing and baking requirements, high tritium inventory, poor oxidation resistance, short sputtering lifetime in Technology Phase of ITER, can not be plasma sprayed in-situ, redeposited material is unlike parent material, large loss of conductivity with neutrons, large neutron swelling, and explosive dust potential. Disadvantages of beryllium include: low melting point, chemical toxicity, self-sputtering > 1 (?), high Young's modulus and CTE, poor CTE match with refractory metals, larger vaporization than tungsten, poor oxidation resistance above 800°C, large neutron swelling and embrittlement, short sputtering lifetime in Technology Phase of ITER, and explosive dust potential. Disadvantages of tungsten are: high Z, potential for severe plasma contamination, surface microcracks after thermal shock, brittle at 25°C, poor CTE match with copper, thicker melt layer than beryllium, high radioactivity hazard, poor oxidation resistance above 600°C, poor waste management, high decay afterheat, neutron embrittlement, and explosive dust potential. Since each material has many disadvantages, it is important to study alternate materials, such as beryllium carbide, boron carbide, or composites of beryllium, boron, and carbon.

Thermal conductivity is an especially critical property because armor tiles must be sufficiently thick to withstand erosion from sputtering and repeated plasma disruptions, as well as protect the heat sink from runaway electrons. Fig. 4 shows 1-D ABAQUS [16] finite element results for the maximum tile thickness at a heat flux of 15 MW/m^2, assuming an allowed (steady-state) surface temperature of 1100°C for carbon and tungsten, and 900°C for beryllium. A large range of thicknesses is evident, from 2 mm for tungsten brazed to niobium, to 20 mm for CAPG brazed to copper.

Materials for the heat sink include: copper alloys, molybdenum–rhenium alloys, and niobium alloys. Disadvantages of copper alloys include: low melting point,

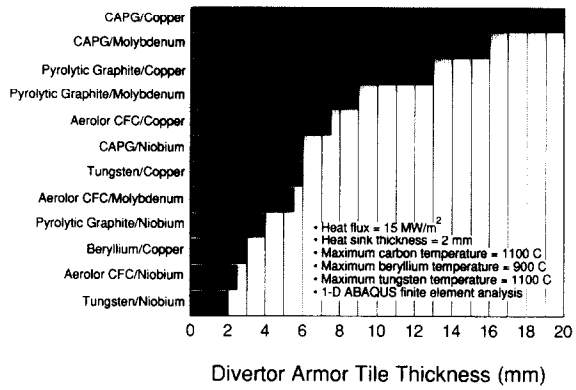

Fig. 4. Maximum allowable tile thickness for divertor element at a steady-state heat flux of 15 MW/m^2 based on 1100°C limit for carbon and tungsten, and 900°C limit for beryllium.

short time to melting after a loss of cooling accident (LOCA), high electrical conductivity, poor CTE match with carbon and tungsten, aqueous erosion/corrosion, high neutron activation, and activated corrosion products. Disadvantages of molybdenum-rhenium alloys include: lower thermal conductivity, difficult fabrication and welding, poor CTE match with beryllium, rapid neutron embrittlement, oxidation at elevated temperatures, high neutron activation, poor long term waste management, expensive, safety hazards with rhenium additions (volatility, activation), and a small HHF data base. Disadvantages of niobium alloys include: low thermal conductivity, poor CTE match with beryllium, poor long term waste management, high tritium permeation, and a small HHF data base. Obviously, continued research and development is needed on all of these materials combinations because a clear "winner" can not be chosen at this time.

5. Thermal-hydraulics

High velocity, highly subcooled water is the preferred coolant for HHF components because it provides a larger heat transfer coefficient than either helium gas or liquid metals [13]. The efficiency of heat transfer is increased by allowing subcooled nucleate boiling, which occurs at fluxes greater than about 10 MW/m^2. In this regime, no net water vapor is generated because the micro-bubbles collapse in the subcooled bulk fluid, thereby creating a highly turbulent boundary layer which enhances heat transfer. Typical values of the heat transfer coefficient are 4 W/cm^2 K for forced convection and 10–15 W/cm^2 K for boiling conditions. Inlet con-

ditions are: temperature 40–80°C, pressure 1–4 MPa, velocity 5–15 m/s, and diameter 8–15 mm. Further enhancements in heat transfer rates can be achieved by modifying the inner surface of the cooling channel with porous or roughened surfaces, internal fins (straight or spiraled), twisted tape inserts, and tangential injection [14,15]. Factors of 2–3 increase in the heat transfer film coefficient can be obtained in the convection regime, with a corresponding increase in the pressure drop and pumping power.

Two and three dimensional finite element computer codes have been used to model the heat transfer in high heat flux components [9]. However, numerical instabilities are often encountered when working in the boiling regime. Some finite element codes, such as ABAQUS [16], have been modified to permit calculation of the non-linear boiling film coefficient in a self-consistent manner with stable solutions. These codes predict that internal heat flux magnification can be as high as 1.8, for circular cooling channels because of geometric focussing. On the other hand, use of copper internal fins can reduce the internal heat flux by as much as 50% because of the extended area in contact with the water. Rectangular cooling channels typically have no effect on the internal heat flux.

Unlimited increases in heat transfer rates can not be achieved with boiling water because of the transition from nucleate boiling to film boiling (also called dryout, or the Leidenfrost effect), which occurs at a critical heat flux (CHF) level. This sudden event occurs when so many bubbles are being generated that a vapor blanket covers the inside surface and insulates the boundary, causing "burnout" and water leakage. A significant number of correlations have been used to predict CHF limits for uniform heating, including: Tong, W-2, Gunther, Gambill, Katto, Bowring, Knoebel, Macbeth, Griffel, and Weisman [17]. CHF predictions range from 20–30 MW/m^2 for a smooth tube with a diameter of 10 mm, a velocity of 10 m/s, a pressure of 2 MPa, and no enhancement. These correlations agree only within a factor of 10 because they require extrapolations to conditions (one-sided heating, high subcooling, etc.) outside the range of experimental data. Nevertheless, fig. 5 shows that good agreement has been found with the Tong correlation for electron beam (one-sided) test data [18]. Japanese results using an ion beam shows better agreement with the Wiesmann–Pei correlation [19], although there should be small differences between ion-beams and electron-beams since both produce essentially a surface heat load. Using a twisted tape insert can increase the CHF limit by a factor of 1.8, to 60 MW/m^2 at 10 m/s with a 10 mm diameter tube [20]. However, Japanese e-beam data indicates a limit of only 40 MW/m^2 with a twisted tape insert at 13 m/s [21]. This may be an effect of using thick walled tubes and using the peak external heat flux, instead of using the (more correct) peak internal heat flux. More experiments are needed to study the effects of heated length,

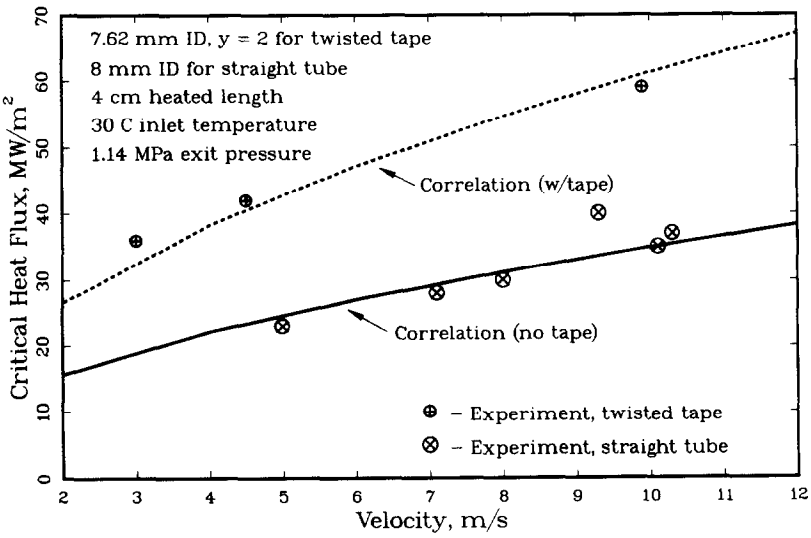

Fig. 5. Comparison of electron beam one-sided critical heat flux measurements with Tong-1975 correlation with and and without twisted tape insert.

inlet temperature, velocity, pressure, internal fins porous coatings, and twist ratio. Use of alternate coolants, such as helium gas, would eliminate the problems of exceeding a critical heat flux limit, however, at the expense of a lower heat transfer coefficient and higher temperatures.

Because the consequences of a water leak in a radioactive machine with tritium are so severe, it is important to have a large burnout safety margin. A safety margin of 4 is recommended because of uncertainties in edge plasma parameters, toroidal field ripple, burn control fluctuations, single/double-null operation, loss of null point sweeping, toroidal facets, support misalignment, thermal distortions, leading edges at gaps, changes in surface topography from erosion or redeposition processes, missing tiles, and neutron swelling and creep deformations. Missing tiles can be caused by runaway electrons, braze defects, or poor quality control. A single missing tile in the strike point area will double the power load on the adjacent tile directly behind the missing one. This results in twice the surface temperature (which may cause a carbon bloom) and twice the internal heat flux (which may cause burnout of the cooling channel). If the adjacent tile subsequently fails, then the power load triples, and so on. The heat flux on the tile's corner can increase by a factor of 30 for an angle of incidence of 2°. Therefore, using a safety margin of 4, and a CHF of 40–60 MW/m^2, this limits the design heat flux to 10–15 MW/m^2.

6. Thermo-mechanics

The largest stresses in high heat flux components are thermal stresses caused by differential thermal expansion. When bending is constrained, the yield stress is often exceeded and cyclic plastic strains can initiate fatigue cracks. Strong thermal shocks can fracture brittle graphite tiles. Carbon/carbon composite tiles have a sufficiently large fracture toughness that sublimation limits are reached before fracturing [22–24]. Primary stresses are generally much smaller due to small diameters and relatively low pressures.

Residual braze stresses can fracture graphite tiles that are brazed to metal substrates because of the large mismatch in the coefficient of thermal expansion [25,26]. Fig. 6 shows an example of a fractured graphite-to-metal braze joint. The fracture almost always initiates at the interface near the free edge corner where a stress singularity exists [27]. A variety of techniques can reduce these stresses. One approach is to choose substrate metals which have a low yield strength, such as annealed OFHC copper, so that the stress singularity is bounded. Another is to use long hold times during the furnace cooldown to allow the substrate to creep and relax out residual stresses. Metal substrates with high yield strengths and high creep resistance (Inconel, Molybdenum, ODS copper, etc.) often crack brazed graphite tiles.

Soft compliant interlayers, such as plasma sprayed

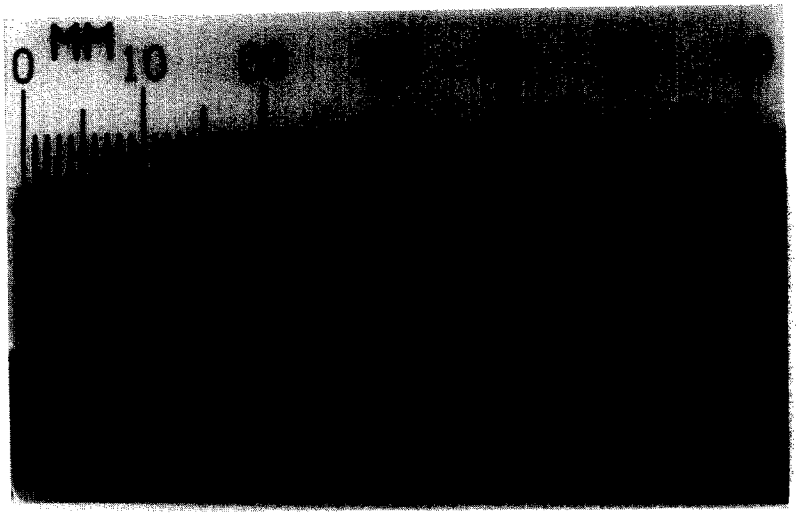

Fig. 6. Braze joint between pyrolytic graphite and OFHC copper showing crack in graphite tile initiating at free edge corner after furnace cool-down due to braze residual stresses.

OFHC copper and copper feltmetal meshes, have successfully been used to braze pyrolytic graphite to high strength copper alloys. Heat transfer through the feltmetal mesh, is limited because of its porosity. Carbon fiber reinforced copper matrix composite interlayers have been used [28], and wrapping copper tubes with either tungsten or carbon fibers is another method being studied. Furthermore, stress analyses have shown that reducing the angle between the free edge and interface to less than 70° eliminates the stress singularity for graphite and copper joints [29]. Slots machined in the soft copper interlayer leave thin connecting webs that can deform and reduce the stress concentration, as well. Graded plasma sprayed coatings have been successfully used to make thick coatings, such as SiC and aluminum [30].

High heat flux testing of beryllium tiles and OFHC copper heat sinks have demonstrated that very long fatigue lifes can be achieved even at heat fluxes that cause elastic stresses which are 3–4 times larger than the yield stress, because the cyclic plastic strains were small, < 1% [31]. An OFHC copper neutral beam dump was operated at 50 MW/m^2 for over 25 000 cycles with 5 s pulses without a water leak [32]. Another OFHC beam dump was operated at 40 MW/m^2 for 10 000 cycles with 20 s pulses without failure [33]. Slotting of the plasma facing surface has been successfully used on both the ISX-B and JET beryllium limiter tiles to delay the initiation of thermal fatigue cracking. High cycle fatigue tests are needed for the less ductile metals, such as molybdenum alloys.

The thermo-mechanical performance of duplex structures with brazed tiles depends on both the quality of the braze bond, as well as the degree of CTE mismatch. Thermal stresses from normal operation are superimposed on the residual braze stresses, and can exceed the ultimate strength of brittle materials. Fig. 7 shows the remains of a D-III armor tile consisting of a 2 cm thick POCO AXF-5Q graphite tile brazed to a 2 cm thick Inconel substrate with a thin molybdenum interlayer after an explosive thermal stress fracture at a heat flux of 0.5 MW/m^2 applied for 3.5 s [34]. In this case, however, the graphite is still well bonded to the substrate. High heat flux testing of a 5 mm thick tungsten tile at 20–30 MW/m^2 for 1 s pulses caused interface fracture and tile melting after only 360 cycles [35]. In another test, a 2 mm thick plasma sprayed tungsten coating on a copper–beryllium alloy tested at 2.5 MW/m^2 for 20 s pulses fractured after 5000 cycles [36,37].

7. Disruption effects

Plasma disruptions pose a severe threat to plasma facing components because of electromagnetic forces, surface erosion, and runaway electron damage. The thermal quench phase in ITER is 0.1–3 ms and can deposit 10–20 MJ/m^2 of energy, melting or vaporizing significant amounts of material. Fortunately, with a highly segmented divertor design, eddy current forces can be reduced to acceptable levels [9].

Fig. 8 shows the calculated vaporization for carbon, beryllium, and tungsten from a plasma disruption thermal quench on the divertor [18]. Threshold damage energies are 1–3 MJ/m^2 for short pulses. A minimum value is 0.1 mm of material vaporized per disruption. Carbon vaporizes less than tungsten, and tungsten is lower than beryllium. The amount vaporized is not very sensitive to the deposition time over the range 0.1–3 ms. Large differences exist between theory and measurements. Simulation experiments using both laser and

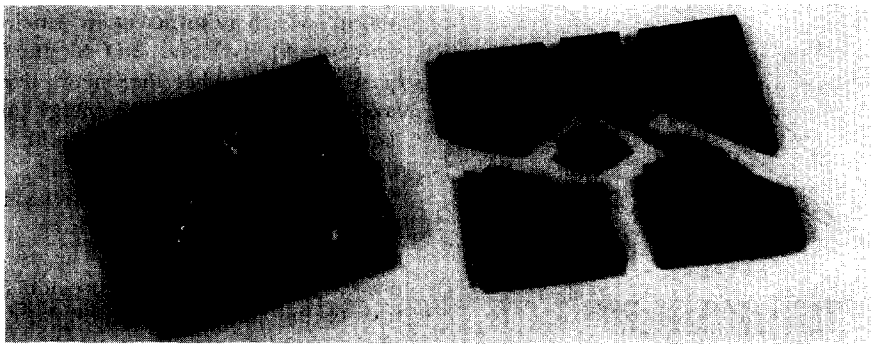

Fig. 7. Thermal stress fracture of POCO AXF-5Q graphite tile brazed to Inconel substrate with 08 mm molybdenum interlayer, after exposure to a heat flux of 0.5 MW/m^2 for 3.5 s.

electron beam irradiations have found that the measured weight loss for carbon exceed the calculated values by factors of 3–6, possibly due to cluster emission of carbon particles [24,38]. In this case, with 10 MJ/m^2 and 0.1 ms deposition, the erosion would increase to 0.5 mm per disruption. Conversely, theoretical models of vapor shielding predict a reduction in the absorbed heat flux by factors of 2–10 (which agree well with some experiments) [39]. In a third experiment with longer pulse lengths (200–500 ms), it was found that the measured weight loss agreed very closely with predictions without having to rely on any vapor shielding effect [40]. If there is a strong effect of pulse length, as the experiments would suggest, then new work being performed in both the USA and USSR using capacitor-type plasma gun discharge units will be very useful.

For beryllium and tungsten, melting thicknesses depend strongly on the deposition time, but not so much on energy above 10 MJ/m^2. Fig. 9 shows a 1-D calculation which shows that tungsten has twice the melt layer thickness than beryllium, despite its high melting point [18]. At 12 MJ/m^2 and 3.0 ms pulse length, the tungsten melt layer is 0.2 mm thick. With higher energies, the melt layer thickness decreases as more energy goes into sublimation. If the melt layer is lost because of surface

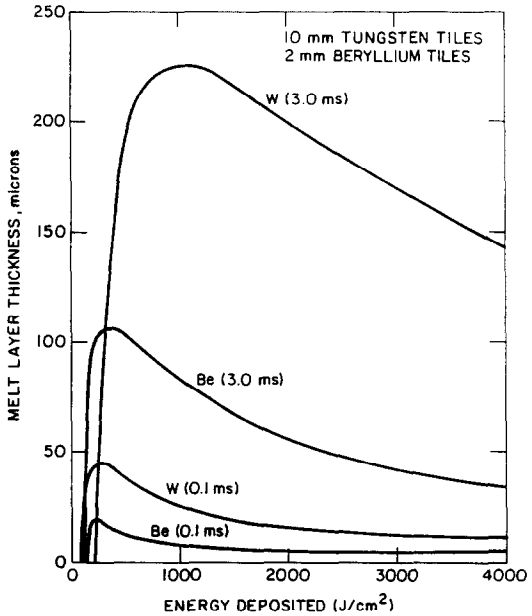

Fig. 9 Calculated amount of material melted during a 0.1 ms plasma disruption for beryllium and tungsten.

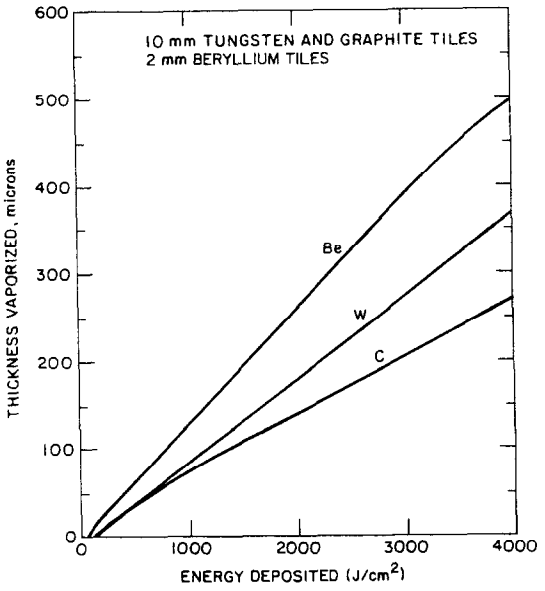

Fig. 8. Calculated thickness of material vaporized as a function of energy deposited for a 0.1 ms plasma disruption.

instabilities, plasma "wind", or electromagnetic forces, then the total disruption erosion is nominally the same between beryllium and tungsten, since beryllium vaporizes roughly 40% more material than tungsten.

Runaway electrons generated during the current quench phase (20–200 ms) of a disruption in tokamaks have been observed to cause severe damage to plasma facing materials, including melting, sublimation, and fractures [41]. For ITER, the maximum electron energy was calculated to be 300 MeV with a flux of 100 MJ/m^2, which is sufficient to penetrate deep into the structure [9]. 1-D and 2-D Monte Carlo codes have been used to predict the energy deposition in multilayered structures [42]. The energy threshold needed to damage the heat sink is roughly 20 MJ/m^2 for copper with 10 mm of carbon armor, at a 5° angle of incidence [9]. Damage thresholds are correspondingly higher for materials with higher melting points, such as molybdenum, and niobium. The use of tungsten as a plasma facing material can provide substantial protection to the water cooled heat sink against runaway electrons. With carbon or beryllium it is difficult to envision how HHF components will survive the high energy runaway electrons that are predicted for ITER.

8. Divertor lifetime issues

In present day fusion devices, the duty cycle is low and component lifetime is generally not a problem. However, for next generation machines, such as ITER or NET, both the pulse length and availability will be high. Because it may require 3–6 months to replace all of the divertor modules in ITER using remote maintenance techniques, a lifetime of one year is a minimum goal.

The sputtering lifetime depends strongly on the plasma edge temperature, angle of incidence, and especially on redeposition [43]. A 4 mm thick graphite divertor tile edge temperature is 150 eV is predicted to have a lifetime of 6 calender months for the Physics Phase of ITER (2% availability) [9]. A 2 mm thick beryllium tile would last only 3 calender months. Tungsten would last several years if the edge temperature was < 40 eV. With the high availability of the Technology Phase, beryllium and carbon lifetimes drop to about one week. Therefore, tungsten appears to be the only material option that gives an acceptable lifetime (if a low edge temperature can be guaranteed).

Erosion by disruptions can also limit the divertor lifetime. Assuming 0.1 mm erosion per disruption, a 10 mm thick carbon composite tile would survive 100 disruptions (less if the 3–6 times enhanced erosion is confirmed or more if vapor shielding is effective). Likewise, for a 3 mm thick beryllium or tungsten tile, the lifetime is predicted to be about 30 disruptions (less if the melt layer is lost). ITER assumes a 5% disruptions frequency (500 disruptions) in the Physics Phase. At this rate, beryllium and tungsten would not be credible options. Plasma spray in-situ repair may alleviate this problem, but there are many unresolved questions regarding the adhesion, thermal conductivity, and thermal shock resistance of the as-deposited material.

9. Safety and reliability

With the use of hazardous materials inside the vacuum vessel (carbon dust, beryllium, tritium, and radioactive structures), safety issues have become a serious issue for fusion devices. Although beryllium is an inhalation hazard, considerable progress has been made at JET in developing procedures for handling beryllium contamination. Release of tritium gas or tritiated water vapor to the environment would be a serious accident. Chemical reactions between air or steam and hot graphite tiles or carbon dust can produce explosive hydrogen gas, carbon monoxide, and mobilize large amounts

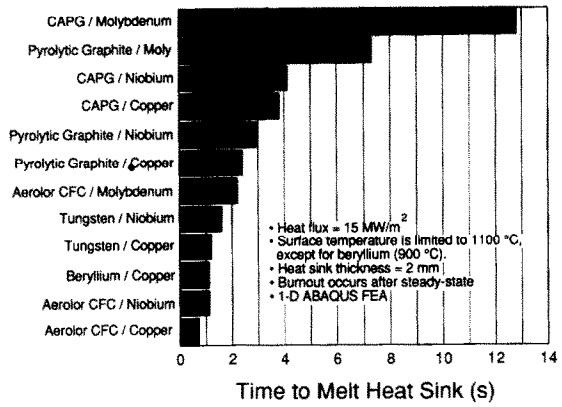

Fig. 10. Calculated time to melt heat sink after a CHF burnout or loss of cooling accident at 15 MW/m^2 without plasma shutdown. Tile thickness for each case is given in fig. 4.

of tritium co-deposited on plasma facing surfaces. A graphite fire could occur in ITER if sufficient air was supplied, under worst-case assumptions [44]. With tungsten coatings, air or steam reactions will oxidize the surface and mobilize radioactive tungsten or rhenium isotopes.

Actively cooled high heat flux components have a very short time to melt during either a CHF burnout event, loss-of-cooling-accident (LOCA), or loss-of-flow-accident (LOFA) because of the thin-walled structure. Fig. 10 shows 1-D ABAQUS [18] finite element results which show that only 1–4 s is needed to melt the heat sink at 15 MW/m^2 if the plasma does not shutdown. The ITER Technology Phase divertor with 2 mm of tungsten brazed to 2 mm of niobium would melt the heat sink in 1.5 s. The survival time can be extended to 12 s by using 20 mm thick tiles made of compression annealed pyrolytic graphite and a molybdenum heat sink. However, if the armor tile is missing, or eroded to less than 1 mm, then the heat sink will melt in less than one s after a LOCA. Also, a single runaway electron event could melt the divertor and cause a massive water leak.

Reliability of cooling tube joints, welds, and armor tile braze bonds must be extremely high. With approximately 500 000 brazed graphite tiles on the ITER divertor, this represents a serious quality control challenge for industry. Present day experience with brazing of approximately 10 000 graphite tiles on water cooled stainless steel for the inner wall of Tore Supra found a failure rate of about 1%. For ITER, this implies 5000 defective braze bonds in the divertor, which would be unacceptable. There is a critical need to develop both

active and passive methods for rapid plasma shutdown, in addition to requiring a large burnout safety margin.

10. Conclusions

The divertor is one of the main performance limiting components for ITER. This paper reviews the critical issues for structures that are designed to withstand heat fluxes > 5 MW/m^2. High velocity, sub-cooled water with twisted tape inserts for enhanced heat transfer provides a critical heat flux limit of 40–60 MW/m^2. Uncertainties in physics and engineering heat flux peaking factors require that the design heat flux not exceed 10–15 MW/m^2 to maintain an adequate burnout safety margin. Armor tiles and heat sink materials must have a well matched thermal expansion coefficient to minimize stresses. The divertor lifetime from sputtering erosion is highly uncertain. The number of disruptions specified for the next fusion device must be reduced to achieve a credible design. In-situ plasma spray repair with thick metallic coatings may reduce the problems of erosion, but questions about adhesion, thermal conductivity, and thermal shock resistance must be answered first. Runaway electrons in ITER have the potential to melt actively cooled components in a single event. A water leak would be a serious accident because of steam reactions with hot carbon, beryllium, or tungsten that could mobilize large amounts of tritium and radioactive isotopes. If the plasma does not shutdown immediately, then the divertor can melt in 1–10 s after a loss of coolant accident. Very high reliability of carbon tile braze joints will be required to achieve adequate safety and performance goals. These critical issues will be addressed in the near future by operation of the Tore Supra pump limiters and the JET pumped divertor. Finally, an accurate understanding of the power flow out of the edge of an DT burning plasma is essential to successful design of optimum high heat flux components.

References

[1] P.M. Anderson et al., Fusion Eng. Des. 9 (1989) 9.
[2] W.B. Gauster, J.A. Koski, and R.D. Watson, J. Nucl. Mater. 122 & 123 (1984) 80.
[3] G. Vieider, M. Harrison, F. Moons, in: Proc. 15th Symp. on Fusion Technology, Utrecht, 1988, p. 125.
[4] F. Moons, et al., in: Proc. 15th Symp. on Fusion Technology, Utrecht, 1988, p. 859.
[5] I. Smid et al., in: Proc. 15th Symp. on Fusion Technology, Utrecht, 1988, p. 1071.
[6] H.E. Kotzlowski, in: Proc. 13th Symp. on Fusion Technology, Varese, 1984, p. 1253.
[7] J. Bohdansky et al., Nucl. Instr. and Meth. B23 (1987) 527.
[8] P.H. Rebut, The Pumped Divertor Proposal, JET Report JET-R (89) p. 16.
[9] R.D. Watson, Ed., ITER Divertor Engineering Design, ITER Report, Max Planck Institute, TN-PC-8-9-1 (October, 1989).
[10] J.B. Whitley and J.A. Koski, in: Proc. 14th Symp. on Fusion Technology, Avignon, 1986, p. 627.
[11] J.A. Koski et al., Proc. 15th Symp. Fusion Technology, Utrecht, 1988, p. 803.
[12] W.B. Gauster, Plasma Facing Materials, Sandia National Laboratories Report, SAND90-0396 (April 1990).
[13] R.D. Boyd, Fusion Technol. 7 (1985) 7.
[14] W.R. Gambil, R.D. Budny and R.W. Wansbrough, J. Chem. Eng. Prog. 57 (32) (1961) 127.
[15] R.D. Boyd, C.P.C. Wong and Y.S. Cha, Technical Assessment of Thermal-Hydraulics for High Heat Flux Fusion Components, Sandia National Laboratories Report, SAND84-0159 (January 1985).
[16] ABAQUS Users Manual, Hibbitt, Karlsson and Sorensen, Inc. (1987).
[17] J.A. Koski et al., in: Proc. National Heat Transfer Conf., Pittsburgh, 1987, Paper No. 87-HT-45.
[18] D. Smith et al., US Contribution to the ITER Plasma Facing Components Engineering Homework Task, ITER Report, Max Planck Institute, TN-PC-1-9-U-1 (June 1989).
[19] H. Nariai and F. Inasaka, Fusion Eng. Des. 9 (1989) 245.
[20] J.A. Koski and C.D. Croessmann, in: Proc. Winter Meeting ASME, Chicago, 1988, Paper No. 88-WA/NE-3.
[21] M. Araki et al., Fusion Eng. Des. 9 (1989) 231.
[22] S. Sato et al., in: Proc. 15th Symp. on Fusion Technology Utrecht, 1988, p. 1078.
[23] C.D. Croessmann et al., Fusion Technol. 15 (1989) 127.
[24] H. Bolt et al., J. Fusion Eng. Des. 9 (1989) 33.
[25] B.J. Dalgleish, M.C. Lu and A.G. Evans, J. Acta Metall. 36 (8) (1988) 2029.
[26] J.P. Blanchard and R.D. Watson, Nucl. Eng. Des./Fusion 4 (1986) 61.
[27] J.P. Blanchard and N.M. Ghoniem, J. Thermal Stresses, 12 (1989) 501.
[28] Y. Gotoh et al., Fusion Eng. Des. 9 (1989) 295.
[29] O.T. Iancu, J. Comput. & Structures (33) (3) (1989) 873.
[30] M.F. Smith, J.B. Whitley, J.M. McDonald, J. Thin Film Solids 118 (1984) 23.
[31] R.D. Watson and J.B. Whitley, Nucl. Eng. Des./Fusion 4 (1986) 49.
[32] S.L. Milora, S.K. Combs and C.A. Foster, Nucl. Eng. Des./Fusion 3 (1986) 301.
[33] J.B. Whitley et al., J. Nucl. Mater. 111 & 112 (1982) 866.
[34] J.G. Watkins et al., Fusion Eng. Des. 9 (1989) 225.
[35] M. Seki, in: Proc. US–Japan Workshop Q-111, La Jolla, CA, February 1990.

[36] M. Seki et al., Fusion Eng. Des. 5 (1987) 205.
[37] M. Ogawa et al., Fusion Eng. Des. 9 (1989) 227.
[38] J.G. Van der Laan, J. Nucl. Mater. 162–164 (1989) 964.
[39] J. Gilligan, D. Hahn and R. Mohanti, J. Nucl. Mater. 162–164 (1989) 957.
[40] C.D. Croessmann, G.L. Kulcinski and J.B. Whitley, J. Nucl. Mat. 141–143 (1986) 108.
[41] K. Hoven et al., J. Nucl. Mater. 162–164 (1989) 970.
[42] K.A. Niemer et al., Modeling of Runaway Electron Damage for the Design of Tokamak Plasma Facing Components, Sandia National Laboratories Report, SAND89-2405 (April 1990).
[43] F. Englemann et al., J. Nucl. Mater. 145–147 (1987) 154.
[44] J. Raeder and S. Piet, Ed., ITER Safety and Environmental Impact – Concepts and Technical Information, ITER Report, Max Planck Institute, TN-SA-9-1 (October 1989).